Improvement in simulation of Eurasian winter climate variability with a realistic Arctic sea ice condition in an atmospheric GCM

Improvement in simulation of Eurasian winter climate variability with a realistic Arctic sea ice condition in an atmospheric GCM

Young-Kwon Lim[1,2], Yoo-Geun Ham[1,3], Jee-Hoon Jeong[4] and Jong-Seong Kug[5]

[1] Global Modeling and Assimilation Office, NASA/GSFC, Greenbelt, MD, USA
[2] I M Systems Group, Goddard Earth Sciences Technology and Research, USA
[3] Goddard Earth Sciences Technology and Research, Universities Space Research Association, USA
[4] Faculty of Earth Systems and Environmental Sciences, Chonnam National University, Korea
[5] Korea Institute of Ocean Science and Technology, Ansan, Korea

E-mail: yoo-geun.ham@nasa.gov

Abstract
The present study investigates how much a realistic Arctic sea ice condition can contribute to improve simulation of the winter climate variation over the Eurasia region. Model experiments are set up using different sea ice boundary conditions over the past 24 years (i.e., 1988–2011). One is an atmospheric model inter-comparison (AMIP) type of run forced with observed sea-surface temperature (SST), sea ice, and greenhouse gases (referred to as Exp RSI), and the other is the same as Exp RSI except for the sea ice forcing, which is a repeating climatological annual cycle (referred to as Exp CSI).

Results show that Exp RSI produces the observed dominant pattern of Eurasian winter temperatures and their interannual variation better than Exp CSI (correlation difference up to ~0.3). Exp RSI captures the observed strong relationship between the sea ice concentration near the Barents and Kara seas and the temperature anomaly across Eurasia, including northeastern Asia, which is not well captured in Exp CSI. Lagged atmospheric responses to sea ice retreat are examined using observations to understand atmospheric processes for the Eurasian cooling response including the Arctic temperature increase, sea-level pressure increase, upper-level jet weakening and cold air outbreak toward the mid-latitude. The reproducibility of these lagged responses by Exp RSI is also evaluated.

Keywords: sea-ice, mid-latitude winter climate, atmospheric GCM

1. Introduction

The sea ice loss during the last few decades is known to have a potential to significantly influence the global climate system, including the Arctic and adjacent high-latitude areas (McBean *et al* 2005, Liu and Alexander 2007, Budikova 2009). Observational evidence in recent studies shows that the sea ice retreat has a cooling impact over the Northern-Hemispheric mid-latitudes (Francis *et al* 2009, Overland and Wang 2010, Jaiser *et al* 2012, Liu *et al* 2012, Outten and Esau 2012). This result, which may seem counterintuitive, suggests the Arctic sea ice plays a complicated role in influencing the boreal winter temperature distribution.
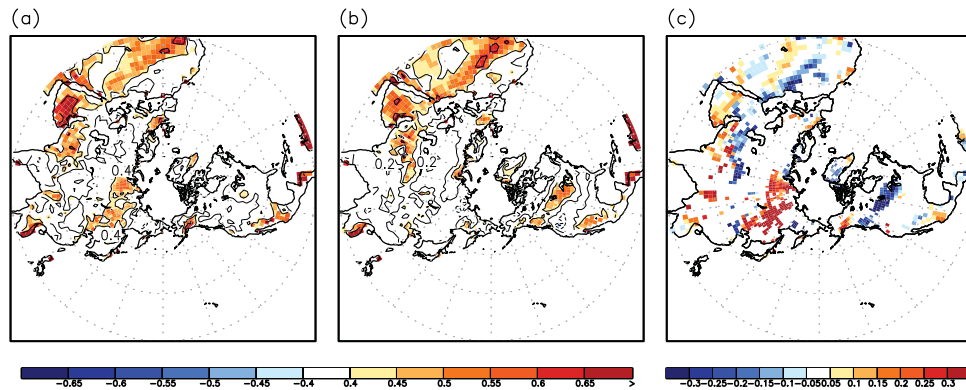
Figure 1. Correlation coefficients of wintertime (DJF) temperatures between the observation and ensemble mean model output in (a) Exp RSI and (b) Exp CSI. The difference, (a) minus (b), is shown in (c). Note that the values that exceed 95% confidence level are shaded in figures 1(a) and (b), and the difference is shaded only where the correlation in either Exp RSI or Exp CSI is over the 95% confidence level.

Model experiments have been widely performed to identify the role of the Arctic sea ice condition in boreal winter. These experiments were done based on the general consensus that the realistic sea ice condition in the model would contribute to the improvement of temperature simulation. These existing model studies mainly focused on a few selected cases (Honda *et al* 1999, Alexander *et al* 2004, Bhatt *et al* 2008, Kumar *et al* 2010, Sedláček *et al* 2012), many of which are either low ice years, or based on climate change projections (Singarayer *et al* 2006, Deser *et al* 2010, Vavrus *et al* 2012). However, improvement of model performance under realistic sea ice conditions will be more rigorously measured if we consider a sufficiently long-term period, which would include various Arctic sea ice conditions, during the recent decades. This approach will also be more helpful for discussing actual predictability under the realistic sea ice conditions. In addition to the predictability issue, regional difference in terms of sensitivity of atmospheric response in the mid-latitude to the Arctic sea ice condition is not well understood.

To address these issues, we investigate how much the realistic Arctic sea ice condition in a model can contribute to a better simulation of the winter temperature variation, as opposed to the climatological sea ice condition. We use an atmospheric general circulation model (AGCM) to perform two types of experiment for the recent past 24 year period from 1988 to 2011 under two different Arctic conditions (i.e., realistic sea ice versus a repeating climatological sea ice cycle). We will focus on the Eurasia region, where the response to the Arctic sea ice retreat is proposed to be relatively strong (Liu *et al* 2012, Outten and Esau 2012). We examine the observed time-lagged responses in the atmosphere to the Arctic sea ice variation, followed by discussion on the model's reproducibility of stronger cooling response over Eurasia than the other mid-latitude areas. We expect that the present study also gives useful insight for reliable seasonal prediction of Eurasian winter temperature variation.

2. Data and model

We use the observational sea ice data archived at the UK Met Office Hadley Centre (Rayner *et al* 2003), and the reanalysis dataset from the Modern Era Retrospective analysis for Research and Applications (MERRA) that was produced by the NASA Goddard Earth Observing System Data Assimilation System Version 5 (GEOS-5). The variables used include surface air temperature, sea-level pressure (SLP), and 200 hPa zonal wind. The winter seasonal mean (DJF) is produced at a horizontal resolution of $0.5° \times 0.6667°$ for the period 1988/89–2011/12.

For the model experiments, we use the NASA GEOS-5 AGCM (Rienecker *et al* 2008). The model is run with 72 hybrid-sigma vertical levels, extending to 0.01 hPa, and ~0.5° horizontal resolution. Two types of experiment are carried out to investigate the impact of sea ice on the boreal winter temperature variation. One is the atmospheric model inter-comparison (AMIP) type of run forced by the observed sea-surface temperature (SST) of HadISST (Rayner *et al* 2003), sea ice, and greenhouse gases (hereafter referred to as Exp RSI), and the other is the same as Exp RSI except for a repeating climatological annual cycle in sea ice (hereafter referred to as Exp CSI). Each type of experiment consists of three ensemble members. All simulations are done with prescribed forcing from early 1988 to 2012. We then analyze the outputs for the 24 DJF periods from 1988/89 to 2011/12.

3. Results

Figure 1 shows the correlation of surface temperatures for wintertime between observations and ensemble-averaged model output. Both experiments produce higher correlations over northern Africa, the Middle East and Mexico relative to the other regions. The area where Exp RSI explains the temperature variability significantly better than Exp CSI is eastern Eurasia, covering eastern Siberia, Mongolia and northeastern China (80°E–140°E, 40°N–75°N; figure 1(c)). This gives some indication that the realistic sea ice distribution in the model is essential for high predictability of winter
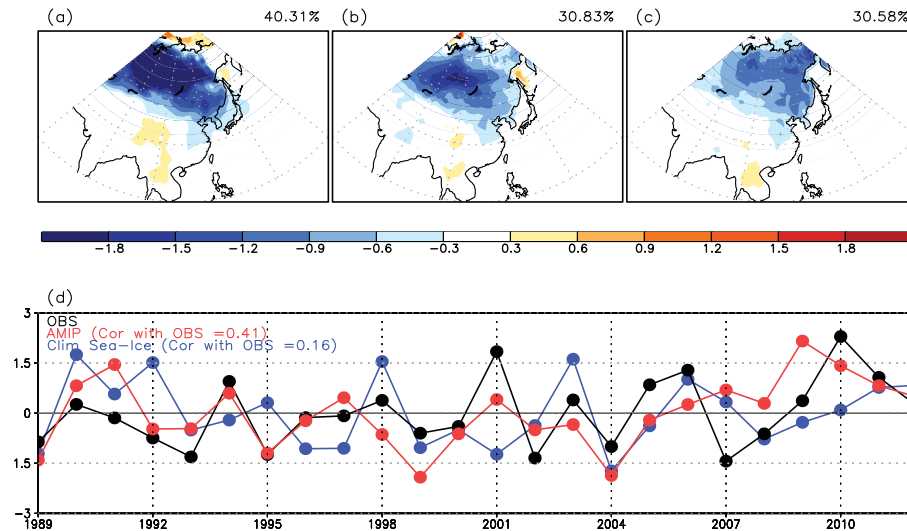
Figure 2. The first EOF eigenvector of DJF surface temperature over 60–160°E, 10–80°N using (a) observations, (b) ensemble mean values in Exp RSI and (c) ensemble mean values in Exp CSI. The corresponding PC time series is shown in (d).

climate over eastern Eurasia. The western Eurasia region shows marginal improvement that does not exceed the statistical significance limit. In contrast, there are several other mid- to high-latitude regions that display higher correlations by Exp CSI (i.e., northeastern Russia near the Kamchatka peninsula, and southern Canada, which includes the Great Lakes). These areas show relatively low correlations in Exp RSI (figure 1(a)), implying weak impact of realistic Arctic sea ice on their winter temperature variations. The observed correlation features in figure 3(c) also represent weak relationship between temperature variability over southern Canada (including the Great Lakes) and the Arctic sea ice variation, compared with the Eurasia region.

To examine how the correlation skill is improved over Eurasia, we perform the EOF analysis to identify the dominant variability over Eurasia. The upper panel in figure 2 shows the first EOF eigenvector distribution that explains the largest temperature variability over eastern Eurasia. The corresponding principal component (PC) time series are plotted in the bottom panel. The explained variance of the first EOF is about ∼31% for the two model experiments and ∼40% for the observations. We find that the distribution of negative anomalies over the area of 60°E–140°E and 40°N–70°N in Exp RSI (pattern correlation with observation: 0.84) is more similar to the observed one than that in Exp CSI (pattern correlation with observation: 0.72). Also, the PC time series in Exp RSI is better correlated to the observed one than that in Exp CSI (i.e., 0.41 for Exp RSI, versus 0.16 for Exp CSI; the significance limit is ∼0.40 at 95% confidence). Further analysis of the second and third EOF modes in Exp CSI reveals no correlation with the first EOF pattern of the observation (not shown). These different features between the two experiments demonstrate that the realistic Arctic sea ice condition is essential for more reliable simulation of temperature patterns and their interannual variation in this region.

To identify the specific region where the sea ice condition is closely connected to the eastern Eurasian winter temperature, correlation is calculated between the observed DJF sea ice concentration and the first EOF PC (upper panels in figure 3). Note that the positive (negative) sign of the PC represents the cold (warm) temperature anomaly over eastern Eurasia. The correlation with Exp CSI is not shown because it is negligible in most regions. The upper panels of figure 3 clearly show that the first EOF PCs from the observation (figure 3(a)) and Exp RSI (figure 3(b)) are both positively correlated with the sea ice over the Arctic Sea, including the Laptev Sea, East Siberian Sea and Beaufort Sea, while the strong negative correlation is observed over the Barents Sea and Greenland. This pattern indicates that the cold anomaly over eastern Eurasia may be related to sea ice expansion over the Siberian Arctic and/or sea ice retreat near the Barents and Kara seas.

Outten and Esau (2012) suggested that the sea ice reduction over the Kara Sea area has a particularly strong impact on mid-latitude temperatures. Based on this understanding, we further analyze the interannual sea ice variation over the Greenland Sea, Barents Sea and Kara Sea, and explore their relationship with the Northern-Hemispheric temperature. The lower panel in figure 3 shows the correlation of the temperature over the Northern Hemisphere with the sea ice concentration index, which considers the sea ice cover near the Barents and Kara seas. The sea ice concentration index is defined as the total area as a percentage with sea ice concentration higher than 25% over the domain that ranges from 60°W to 60°E and from 65°N to 90°N. Figures 3(c) and (d) show a covariance between warm (cold) anomalies over Greenland and less (more) than normal sea ice in the Barents and Kara sea. In addition, there is a wide area of strong positive correlation in mid-latitude Eurasia, indicating that sea ice increase (decrease) has a warming (cooling) impact (figure 3(c)). This positive correlation throughout mid-latitude
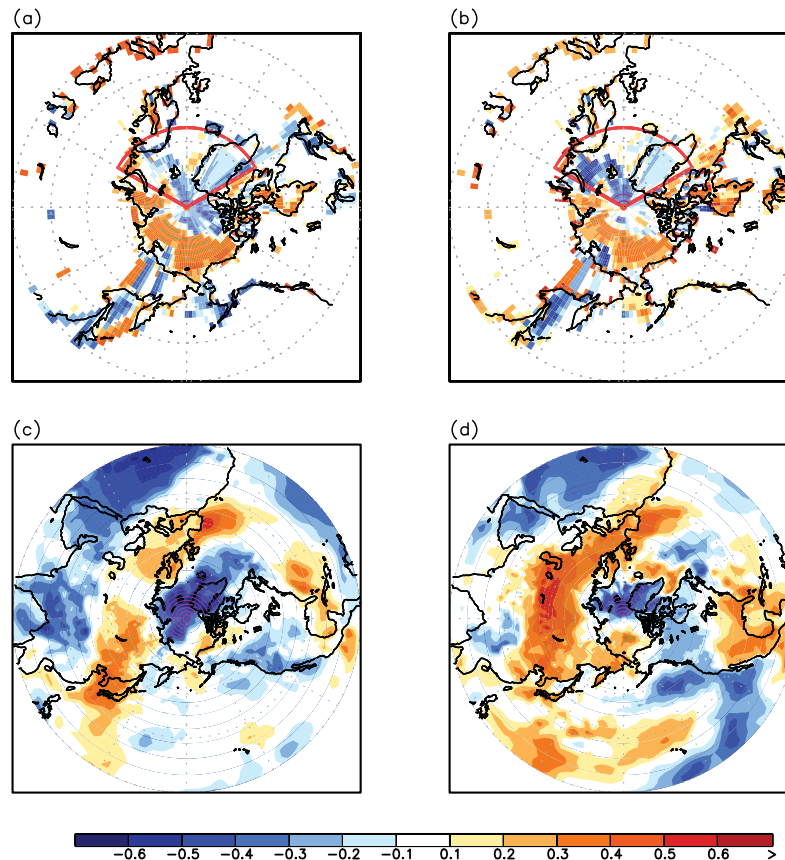
Figure 3. (a) Correlation coefficient between observed sea ice concentration and the first EOF PC time series of observations. (b) The same as (a), except the PC time series is from Exp RSI. (c) Correlation coefficients between observed sea ice concentration index and observed surface temperature. Note that the sea ice concentration index is defined as the total area as a percentage with sea ice concentration higher than 25% over the domain with the boundary ranging from 60°W to 60°E and from 65°N to 90°N, and denoted as a red box in panels (a) and (b). (d) The same as (c), except the surface temperature is from Exp RSI. The green and purple dots denote the 95% confidence level.

Eurasia is successfully identified in Exp RSI (figure 3(d)), with greater correlation values than those in the observation (figure 3(c)). A similarity in the correlation pattern between figures 3(c) and (d) indicates a realistic simulation of interannual temperature variation via the realistic Arctic sea ice condition in the model (Liu *et al* 2009, Outten and Esau 2012).

While the recent studies explained the mechanism for the cold winter in response to the sea ice retreat (Francis *et al* 2009, Higgins and Cassano 2009, Deser *et al* 2010, Overland and Wang 2010, Jaiser *et al* 2012, Liu *et al* 2012, Outten and Esau 2012), their main focus on the time-lagged responses lies in the winter time temperature response to the sea ice condition in the summer or fall season. The range of the dominant time lag for atmospheric responses to the winter sea ice condition and its impact during the following spring are yet to be discussed. Thus, we examine the sequence of time-lagged responses of the atmospheric variables and Eurasian surface air temperature to the Arctic sea ice variation in winter. To do this, surface air temperatures, SLP, and upper-level westerly are regressed onto the Arctic sea ice index time series in consideration of time lag from −2

months (i.e., November) through +3 months (i.e., April) from January. The sea ice concentration index for the DJF season is used as a proxy to find out not only the dominant time period that influences the Eurasian temperature but also the effectiveness of the winter sea ice condition.

The left panel in figure 4 shows the lagged response of the observed surface air temperature, SLP, and upper-level jet to the Arctic sea ice reduction over the Barents and Kara seas. The contours in figure 4(a) denote the temperature averaged over the zonal band of 60°W and 60°E, which is close to the zonal band of the Barents and Kara sea area, while the temperature averaged over the band of 60°E and 140°E is shaded to reflect the Eurasian region. The temperature in the Arctic region (say north of 70°N) tends to respond quickly to the sea ice reduction as the temperature maximum appears at zero-month lag. However, the mid-latitude area from 40°N to 70°N exhibits clear time-lagged responses, reaching the maximum negative temperature anomaly at one-month lag. In order to find out how this lagged response in the Eurasian mid-latitude is feasible, the associated response of SLP and upper-level westerly is calculated (figures 4(d), (g)). It clearly shows that SLP increase at high latitude takes place
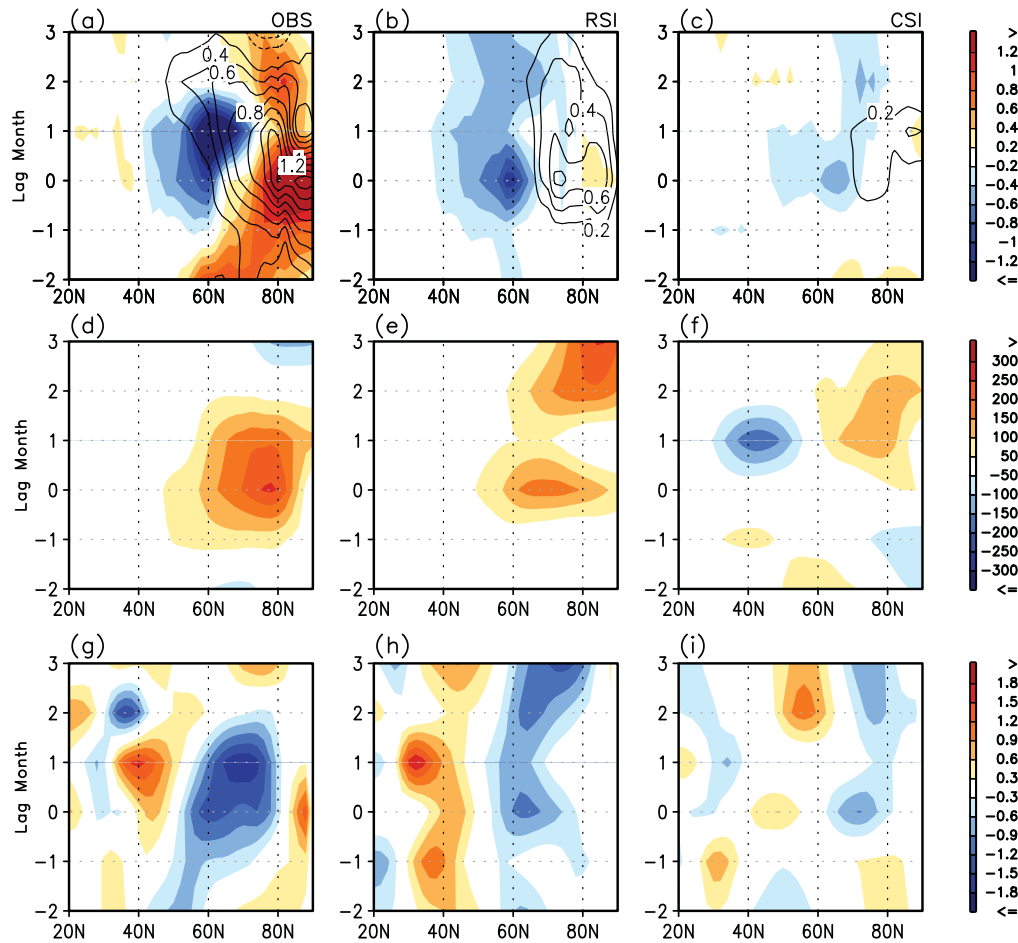
Figure 4. Time (lag)–latitude section of the lag-regressed anomalies onto the observed sea ice concentration index. The upper panels show the lag-regressed surface temperature anomaly (K) in (a) observations, (b) Exp RSI, and (c) Exp CSI from −2 months (i.e., November) through +3 months (i.e., April) from January. The contours denote the temperatures averaged over the zonal band of 60°W and 60°E, while the averaged values over the band of 60°E and 140°E are shaded to reflect the Eurasian region. The middle and lower panels are the same as the upper panels, except for sea-level pressure (SLP) (hPa) and zonal wind at 200 hPa (m s^{-1}).

dominantly from zero- to one-month lag, with relatively more prominence at zero-month lag. This SLP increase can be understood by temperature increase at high latitude (Royer *et al* 1990, Budikova 2009). Compared with the SLP response, upper-level westerly jet weakening in the 60°N–80°N is clearer at one-month lag than at zero-month lag. This indicates that the weakening of the upper-level jet appears after the SLP increase plays a role in weakening the meridional thermal gradient in the equivalent-barotropic structure (Royer *et al* 1990, Outten and Esau 2012). These atmospheric responses lead to the maximum cooling in the Eurasian mid-latitude at about one-month lag. The observation also explain that impact of the Arctic sea ice reduction in winter may not be strong enough to cause a cooling response in the Eurasian mid-latitude in the following spring, although the warming response in the Arctic (red shadings) persists throughout the following spring.

The reproducibility of these observed time-lagged responses in the model is evaluated. The anomalous structure in the atmosphere and resulting temperature anomaly over

Eurasia are apparently better simulated by Exp RSI (middle panel) than Exp CSI (right panel). A series of responses, that is, Arctic temperature increase, SLP increase, upper-level jet weakening and cooling in the Eurasian mid-latitude, are better captured in Exp RSI. However, the time-lagged responses found in the observation do not appear to be reasonably reproduced by any model experiments. The strongest response in the model is at zero-month lag, while the observation shows one-month lag. This might be the reason for the overestimated correlations over Eurasia in the model seen in figure 3(d). This faster response in the simulation (figure 4(b)) than in the observation (figure 4(a)) may be also associated with very sensitive atmospheric response to the oceanic boundary condition in the model.

We additionally investigate the time-lagged responses to the summer/fall sea ice condition. The observed winter temperature anomaly is also better reproduced by Exp RSI than by Exp CSI, supporting the view that better representation of sea ice in a model could improve the

predictability in winter temperatures over Eurasia (figure not shown).

4. Concluding remark

The main focus of the present study is to quantify the degree of importance of the Arctic sea ice condition to the simulation of remote atmospheric response in the Northern Hemisphere. We have shown that realistic sea ice variation in the model makes a significant contribution to improvement in the simulation of interannual temperature variation in Eurasia for the last 24 winters. The improvement is more prominent over the Eurasian mid-latitude than the other Northern-Hemispheric regions. This implies that realistic sea ice is one of the crucial factors to realistically simulate mid-latitude winter climate. We also investigated the sequence of time-lagged responses of the atmospheric variables to the Arctic sea ice variation in winter. The one-month lagged cooling response over Eurasia is dominant with the sea ice reduction during winter. The results in Exp RSI show that the simulated atmospheric responses are generally reasonable, even though the response in the mid-latitude is faster than that observed. However, our results are based on the experiments using a single AGCM; therefore, further analysis should be carried out to assess the generalness of these conclusions using other AGCMs.

Acknowledgments

References

Alexander M A, Bhatt U S, Walsh J E, Timlin M S, Miller J S and Scott J D 2004 The atmospheric response to realistic Arctic sea ice anomalies in an AGCM during winter *J. Clim.* **17** 890–904

Bhatt U S, Alexander M A, Deser C, Walsh J E, Miller J S, Timlin M S, Scott J and Tomas R A 2008 The atmospheric response to realistic reduced summer Arctic sea ice anomalies *Arctic Sea Ice Decline: Observations, Projections, Mechanisms, and Implications* (*Geophysical Monograph Series* vol 180) (Washington, DC: American Geophysical Union) pp 91–110

Budikova D 2009 Role of Arctic sea ice in global atmospheric circulation: a review *Glob. Planet. Change* **68** 149–63

Deser C, Tomas R, Alexander M and Lawrence D 2010 The seasonal atmospheric response to projected Arctic sea ice loss in the late twenty-first century *J. Clim.* **23** 333–51

Francis J A, Chan W, Leathers D J, Miller J R and Veron D E 2009 Winter Northern Hemisphere weather patterns remember summer Arctic sea-ice extent *Geophys. Res. Lett.* **36** L07503

Higgins M E and Cassano J J 2009 Impacts of reduced sea ice on winter Arctic atmospheric circulation, precipitation, and temperature *J. Geophys. Res.* **114** D16107

Honda M, Yamazaki K, Nakamura H and Takeuchi K 1999 Dynamic and thermo-dynamic characteristics of atmospheric response to anomalous sea-ice extent in the Sea of Okhotsk *J. Clim.* **12** 3347–58

Jaiser R, Dethloff K, Handorf D, Rinke A and Cohen J 2012 Impact of sea ice cover changes on the Northern Hemisphere atmospheric winter circulation *Tellus* A **64** 11595

Kumar A, Perlwitz J, Eischeid J, Quan X, Xu T, Zhang T, Hoerling M, Jha B and Wang W 2010 Contribution of sea ice loss to Arctic amplification *Geophys. Res. Lett.* **37** L21701

Liu Z and Alexander M 2007 Atmospheric bridge, oceanic tunnel, and global climate teleconnections *Rev. Geophys.* **45** RG2005 RG000172

Liu J, Curry J A, Wang H, Song M and Horton R M 2012 Impact of declining Arctic sea ice on winter snowfall *Proc. Natl Acad. Sci.* **109** 4074–9

Liu Y, Key J R and Wang X 2009 Influence of changes in sea ice concentration and cloud cover on recent Arctic surface temperature trends *Geophys. Res. Lett.* **36** L20710

McBean G, Alekseev G, Chen D, Forland E, Fyfe J, Groisman P Y, King R, Melling H, Vose R and Whitfield P H 2005 Arctic climate: past and present *Arctic Climate Impact Assessment* (Cambridge: Cambridge University Press) pp 21–60

Outten S D and Esau I 2012 A link between Arctic sea ice and recent cooling trends over Eurasia *Clim. Change* **110** 1069–75

Overland J E and Wang M 2010 Large-scale atmospheric circulation change are associated with the recent loss of Arctic sea ice *Tellus* A **62** 1–9

Rayner N A *et al* 2003 Global analyses of sea surface temperature, sea ice, and night time air temperature since the late nineteenth century *J. Geophys. Res.* **108** 4407

Rienecker M M *et al* 2008 The GEOS-5 data assimilation system—documentation of versions 5.0.1 and 5.1.0, and 5.2.0 *NASA Technical Report Series on Global Modeling and Assimilation* NASA/TM-2008-104606 27 pp 1–92 (http://gmao.gsfc.nasa.gov/systems/geos5/index_arch.php)

Royer J F, Planton S and Déqué M 1990 A sensitivity experiment for the removal of Arctic sea ice with the French spectral general circulation model *Clim. Dyn.* **5** 1–17

Sedláček J, Knutti R, Martius O and Beyerle U 2012 Impact of a reduced Arctic sea ice cover on ocean and atmospheric properties *J. Clim.* **25** 307–19

Singarayer J S, Bamber J L and Valdes P J 2006 Twenty-first-century climate impacts from a declining Arctic sea ice cover *J. Clim.* **19** 1109–25

Vavrus S J, Holland M M, Jahn A, Bailey D A and Blazey B A 2012 Twenty-first-century Arctic climate change in CCSM4 *J. Clim.* **25** 2696–710